



Hydroformylation of olefins by Au/Co₃O₄ catalysts

Xiaohao Liu ^{a,d}, Baoshan Hu ^b, Kaoru Fujimoto ^b, Masatake Haruta ^{c,d}, Makoto Tokunaga ^{a,d,*}

^a Department of Chemistry, Graduate School of Science, Kyushu University, Higashi-ku, Fukuoka 812-8581, Japan

^b Department of Chemical Processes and Environments, Faculty of Environmental Engineering, The University of Kitakyushu, 1-1 Hibikino, Wakamatsu-ku, Kitakyushu 808-0135, Japan

^c Department of Applied Chemistry, Graduate School of Urban Environmental Sciences, Tokyo Metropolitan University, 1-1 Minami-osawa, Hachioji, Tokyo 192-0397, Japan

^d Japan Science and Technology Agency (JST), CREST, 4-1-8 Honcho, Kawaguchi, Saitama 332-0012, Japan

ARTICLE INFO

Article history:

Received 10 June 2009

Received in revised form 24 July 2009

Accepted 25 August 2009

Available online 29 August 2009

Keywords:

Hydroformylation

Gold catalyst

Cobalt catalyst

1-Hexene

Heterogeneous catalysis

ABSTRACT

The hydroformylation of olefins over supported gold catalysts in an autoclave reactor under mild conditions (100–140 °C, 3–5 MPa) has been studied. Over Au/AC (activated carbon), Au/PVP (polyvinylpyrrolidone), Au/Al₂O₃, Au/TiO₂, Au/Fe₂O₃, Au/ZnO, Au/CeO₂ and Co₃O₄, 1-olefin mainly remained unchanged and the major products were isomerized olefins or hydrogenated paraffin. In contrast, Au nanoparticles deposited on Co₃O₄ led to remarkably high catalytic activities in hydroformylation reaction with selectivities above 85% to desired aldehydes. The hydroformylation of olefins proceeds preferentially at temperatures below 140 °C, above which the reactions of olefins gradually shifted to isomerization and then to hydrogenation. It appeared that the activity and selectivity of hydroformylation reaction strongly depend on the molecular structure of olefins, which could be ascribed to steric constraints as internal olefins are relatively inappropriate to form alkyl group and subsequent acyl group by insertion of CO. The Au/Co₃O₄ catalyst can be recycled by simple decantation with slight decrease in catalytic activity along with an increase in recycle times, which is a great advantage over homogeneous catalysts. The role of gold nanoparticles can be assumed to dissociate hydrogen molecule into atomic species which reduce Co₃O₄ to Co metal under mild reaction conditions.

© 2009 Elsevier B.V. All rights reserved.

1. Introduction

The hydroformylation of olefins with H₂ and CO (1:1 in molar ratio) discovered in 1938 has long been and remains even now an important industrial chemical process [1], which annually produces 7 million ton of aldehydes. They are used for the subsequent manufacturing of plasticizers, surfactants, soaps, and detergents. Notwithstanding a number of advantages over their heterogeneous counterparts such as high accessibility of all catalytic sites and possibility of tuning selectivity, homogeneous catalytic systems have disadvantages in separating the catalyst from the products and in its recycle use [2,3]. In addition, the cost of dominantly used rhodium catalysts are about 4000 times as that of cobalt [1c]. Moreover, the hydroformylation reaction with homogeneous cobalt complex, for example, Co₂(CO)₈ requires rather harsh conditions (syngas pressure >30 MPa) to stabilize the catalyst and to prevent the formation of insoluble higher carbonyl

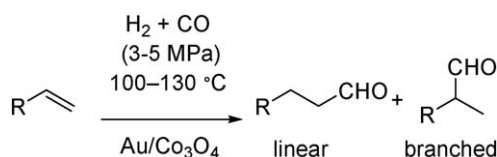
clusters or cobalt precipitates. Both homogeneous carbonyl compounds HCo(CO)₄ and Co₂(CO)₈ are highly toxic.

Thus, solutions to the problems described above are to heterogenize Co⁰ metal or Co⁰ complex catalysts by anchoring the catalyst on a support such as polymer [4–6], activated carbon [7,8], and silica [9–11]. Active sites can be immobilized on the support through chemical or physical interaction to form heterogeneous catalysts to develop economical and environmentally friendly “green processes”. Recently, gold has been proven to be an effective catalytic component for many reactions [12,13]. The most important key is to support nanoparticles of gold on selected metal oxides [14–19] or to design bimetallic structures [20,21]. The fact that gold nanoparticles exhibit markedly high catalytic activity and selectivity by the synergy with the metal oxide supports [22,23] has motivated us to prepare heterogeneous hydroformylation catalysts based on Co₃O₄. Gold nanoparticles deposited on base metal oxides can adsorb CO [24] moderately and are active for CO oxidation, water gas shift reaction [25], olefin hydrogenation [26], and methanol synthesis [27].

In a similar manner to these reactions, for the 70-year-old hydroformylation reaction (Scheme 1), various supported gold catalysts were screened. As a result, the combination of nano-sized Au deposited on Co₃O₄ has shown high catalytic performance for

* Corresponding author at: Department of Chemistry, Graduate School of Science, Kyushu University, Higashi-ku, Fukuoka 812-8581, Japan. Tel.: +81 92 642 7528; fax: +81 92 642 7528.

E-mail address: mtok@chem.kyushu-univ.jp (M. Tokunaga).



Scheme 1. Au/Co₃O₄-catalyzed hydroformylation of 1-olefins.

the hydroformylation of olefins, although neither Au nor Co₃O₄ was active [28].

This work attempts to elucidate the role of gold in the catalytic system composed of Au and Co for hydroformylation reaction. Gold nanoparticles were supported on different supports, AC (activated carbon), PVP (polyvinylpyrrolidone), reducible metal oxide such as TiO₂, Fe₂O₃, ZnO and CeO₂, and insulating metal oxides Al₂O₃, in addition to Co₃O₄. The performance of Co₃O₄-based gold catalysts was studied in detail in relation to the catalyst pretreatment with hydrogen, gold loading, reaction conditions (temperature, reactant pressure), catalyst recycle use, and characterization by means of BET, XRD, TEM, and IR. Furthermore, SiO₂-supported Co or Au-Co

catalysts were also examined for the hydroformylation reaction for investigating the role of gold.

2. Experimental

2.1. Preparation of catalysts

The 5 at.% Au/Fe₂O₃ and 5 at.% Au/ZnO were prepared by co-precipitation at 70 °C followed by calcination in air at 400 °C for 4 h. The 3 wt.% Au/TiO₂ and 5 wt.% Au/CeO₂ were prepared by deposition-precipitation at 70 °C followed by calcination in air at 400 °C for 4 h. The 1.5 wt.% Au/AC was prepared by deposition-reduction followed by calcination in air at 400 °C for 4 h. The 1 wt.% Au/Al₂O₃ was prepared by grinding dimethyl Au(III) acetylacetone with Al₂O₃ powder in a mortar and by calcination in air at 400 °C for 4 h. Colloidal gold nanoparticles stabilized by polyvinylpyrrolidone (Au:PVP) were prepared by reduction of AuCl⁴[−] with NaBH₄ in the presence of PVP [29].

The Au/Co₃O₄ catalyst was prepared by co-precipitation at room temperature to avoid the reduction of gold complex ion with

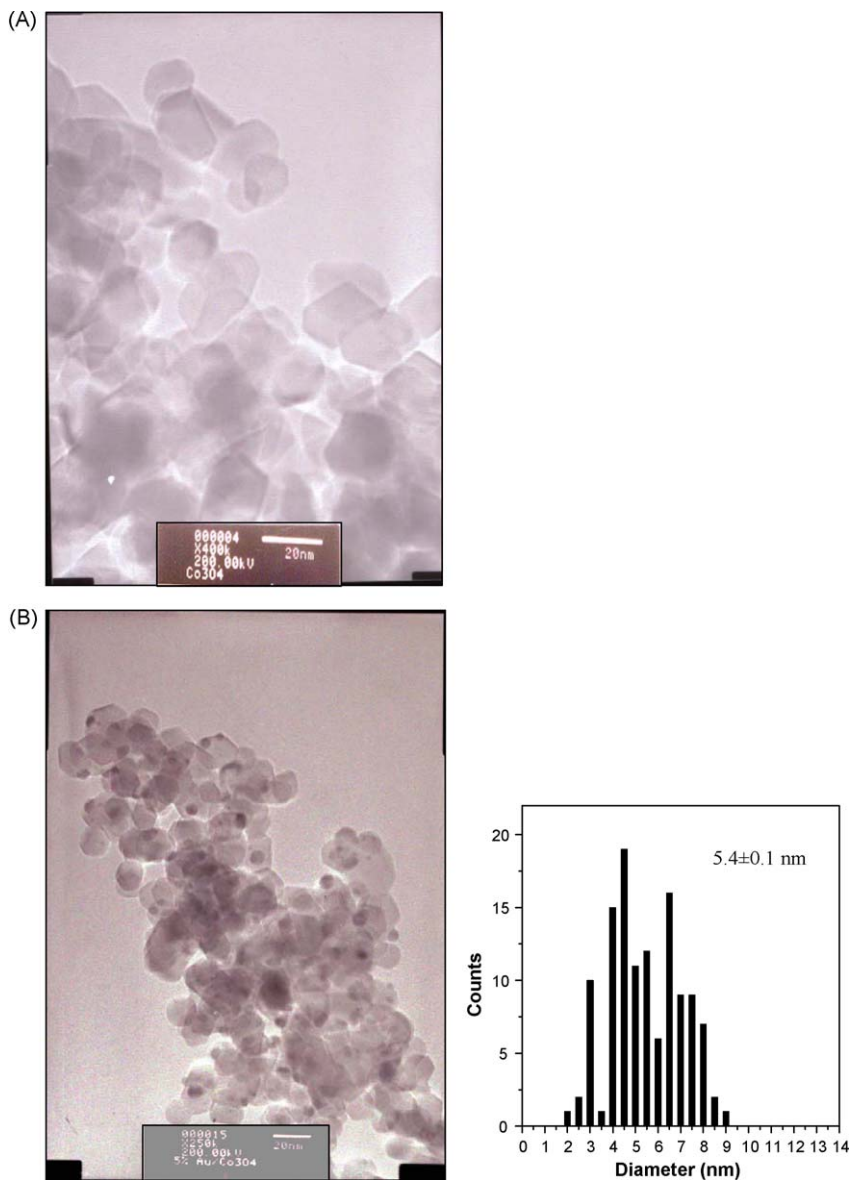


Fig. 1. TEM images and the size distribution of gold particles for Au/Co₃O₄ catalysts with different Au loadings prepared by co-precipitation followed by calcination at 400 °C. (A) Co₃O₄, (B) 5 at.% Au/Co₃O₄, (C) 10 at.% Au/Co₃O₄, (D) 25 at.% Au/Co₃O₄.

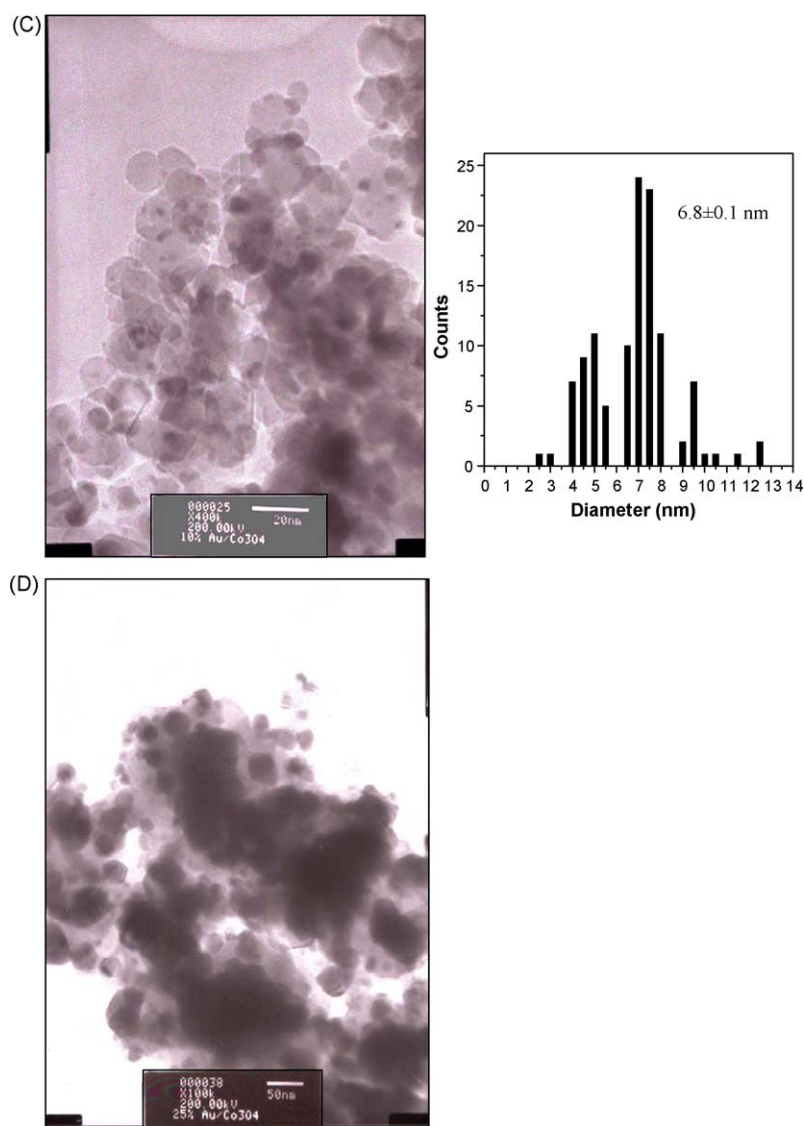


Fig. 1. (Continued).

the oxidation of Co^{2+} to Co^{3+} . Aqueous solution of cobalt(II) nitrate hexahydrate and HAuCl_4 was added to sodium carbonate solution at one time at room temperature. The co-precipitates were washed, dried overnight at 100°C , and calcined in air at 400°C for 4 h. The Co_3O_4 was prepared in the same procedure. The 20 wt.% Co/SiO_2 was prepared from cobalt(II) nitrate hexahydrate and commercially available SiO_2 (Q-15, Fuji Silysia Chemical Ltd.) by an incipient wetness impregnation method using ethanol or aqueous solution. The catalyst precursor was dried overnight in air at 100°C and calcined $\text{Co}_3\text{O}_4/\text{SiO}_2$. Then the dried samples were reduced in a H_2 stream of 40 ml/min at 400°C for 3 h to transform into Co/SiO_2 . The Co-Au/SiO_2 (atom ratio of $\text{Co}:\text{Au} = 19:1$) was prepared by impregnating cobalt(II) nitrate hexahydrate and dimethyl(acetylacetone)gold(III) in ethanol or HAuCl_4 in H_2O by sequential impregnation or co-impregnation method. The following procedures were the same as those for 20 wt.% Co/SiO_2 . The gold loading was expressed by at.% = $100 \times \text{Au}/(\text{Au} + \text{M})$.

2.2. Characterization

Powder X-ray diffraction (XRD) studies were carried out with a RINT 2000 System (Rigaku) diffraction meter using Cu-K_α

radiation. The Brunauer–Emmett–Teller (BET) surface areas and pore volumes were determined from nitrogen adsorption and desorption isotherm data obtained at 77.3 K using an Autosorb-1 apparatus (Quantachrome). The microstructures of calcined samples were studied by transmission electron microscope (TEM) images obtained on a JEM 2100XS instrument (JEOL) operated at 200 kV. Infrared spectra (IR) of reaction mixtures with catalyst were recorded using a React IR-KU 4000 spectrometer (Mettler-Toledo). NMR spectra were recorded on ECS-400 instruments (JEOL). GC analysis was carried out using a GC 6850 (Agilent) equipped with HP-1 Column (J&W, length 30 m, 0.32 mm I.D.) GC-MS analysis was performed with a Polaris Q instruments (Thermo Fisher Scientific) equipped with a Trace TR-5 Column (Thermo Fisher Scientific, length 7 m, 0.32 mm I.D.).

2.3. Catalytic tests for hydroformylation

Hydroformylation was conducted in a 20 ml stainless steel autoclave reactor with a glass tube equipped inside. Reaction temperature was controlled by using an oil bath. The catalyst (20 mg), solvent (14 mmol), and olefin (8 mmol) was introduced into the autoclave in sequence. The autoclave was purged with

syngas ($\text{CO}/\text{H}_2 = 1/1$ in molar ratio) twice and then the pressure was adjusted to a given initial pressure (4 MPa) at room temperature. The mixture was then stirred and the temperature was elevated to reaction temperature. In the case of catalyst pretreatment with hydrogen, the autoclave was charged with solvent (14 mmol) and catalyst (20 mg) and was purged with hydrogen twice. The pressure was adjusted to 2 MPa and reduced the catalyst at 100 °C for 3 h. After pretreatment with hydrogen, the catalyst and solvent was cooled to room temperature and then olefin was introduced to carry out the hydroformylation reaction according to the same procedure as described above. In the case of Co/SiO_2 or $\text{Co}-\text{Au}/\text{SiO}_2$, the catalyst was reduced in a glass tube in a hydrogen flow of 40 ml/min under atmospheric pressure at 400 °C for 3 h. The products of hydroformylation were determined and characterized by GC, GC-MS and NMR.

3. Results

3.1. Catalyst characterization

3.1.1. TEM images

Fig. 1 shows TEM images of the $\text{Au}/\text{Co}_3\text{O}_4$ catalysts prepared by co-precipitation followed by calcination at 400 °C. Irrespective of different gold loadings, Co_3O_4 particles are similar in size at around 20–40 nm, while the size of Au particles changes with gold loadings. Five atom% gold loading leads to a low population of Au nanoparticles with sizes of 3–10 nm on the surfaces of Co_3O_4 . The change in the size of Au nanoparticles for 10 at.% $\text{Au}/\text{Co}_3\text{O}_4$ is not obvious. However, the percentage of larger gold particles (6–10 nm) and the population of gold particles on Co_3O_4 increase. In the case of 25 at.% $\text{Au}/\text{Co}_3\text{O}_4$, the TEM image indicates that the Au seems to give rise to coating-like patterns on Co_3O_4 and may not form clear nanoparticles.

3.1.2. Structural properties

As shown in Fig. 2, the specific surface area and pore structure of catalysts were markedly affected by gold loadings. The specific surface area decreases with an increase in gold loading and is the smallest for 25 at.% $\text{Au}/\text{Co}_3\text{O}_4$, whereas the pore volume and pore diameter reach maxima at 5 or 10 at.% gold loading and are almost similar to each other for Co_3O_4 and 25 at.% $\text{Au}/\text{Co}_3\text{O}_4$.

3.1.3. X-ray diffraction

Fig. 3(a and b) shows XRD patterns of 10 at.% $\text{Au}/\text{Co}_3\text{O}_4$ before and after the treatment with hydrogen in *n*-heptane at 120 °C. The fresh catalyst gives only Co_3O_4 peaks at $2\theta = 19.0^\circ, 31.4^\circ, 36.9^\circ, 44.7^\circ, 55.7^\circ, 59.3^\circ, 65.2^\circ$, and 77.5° and gold peaks at $2\theta = 38.2^\circ, 44.4^\circ, 64.7^\circ$, and 77.6° [30–32]. The XRD patterns for catalyst reduced with hydrogen (2.0 MPa) at 100 °C for 3 h in *n*-heptane are composed of CoO peak at $2\theta = 42.4$ and strong Co^0 peaks at $2\theta = 44.1^\circ, 47.6^\circ$ and 75.9° , but not of Co_3O_4 [30–32].

Fig. 3(c and d) shows XRD patterns of 20 wt.% Co/SiO_2 calcined and reduced in an atmospheric 80 ml/min hydrogen flow at 400 °C for 3 h. The diffraction peaks at $31.3^\circ, 36.8^\circ, 45^\circ, 55^\circ, 59.4^\circ$, and 65.4° are those of Co_3O_4 . After reduction and passivation, most of the cobalt in Co/SiO_2 catalyst existed as Co metal ($2\theta = 44.1^\circ, 51.5^\circ$) and the peaks of CoO were also evident at $36.5^\circ, 42.4^\circ$ and 61.3° . No peaks of Co_3O_4 could be detected due to the complete reduction to CoO or Co metal.

3.1.4. IR spectroscopy

Fig. 4 shows IR spectra of homogeneous $\text{Co}_2(\text{CO})_8$ and heterogeneous $\text{Au}/\text{Co}_3\text{O}_4$ catalytic system. Cobalt carbonyl exhibits a strong peak at 2070 cm^{-1} (Fig. 4a) [33]. After reaction, the catalytic species, $\text{HCo}(\text{CO})_4$, whose characteristic peaks at 2050 and 2030 cm^{-1} are clearly observed (Fig. 4b) [33]. When exposed

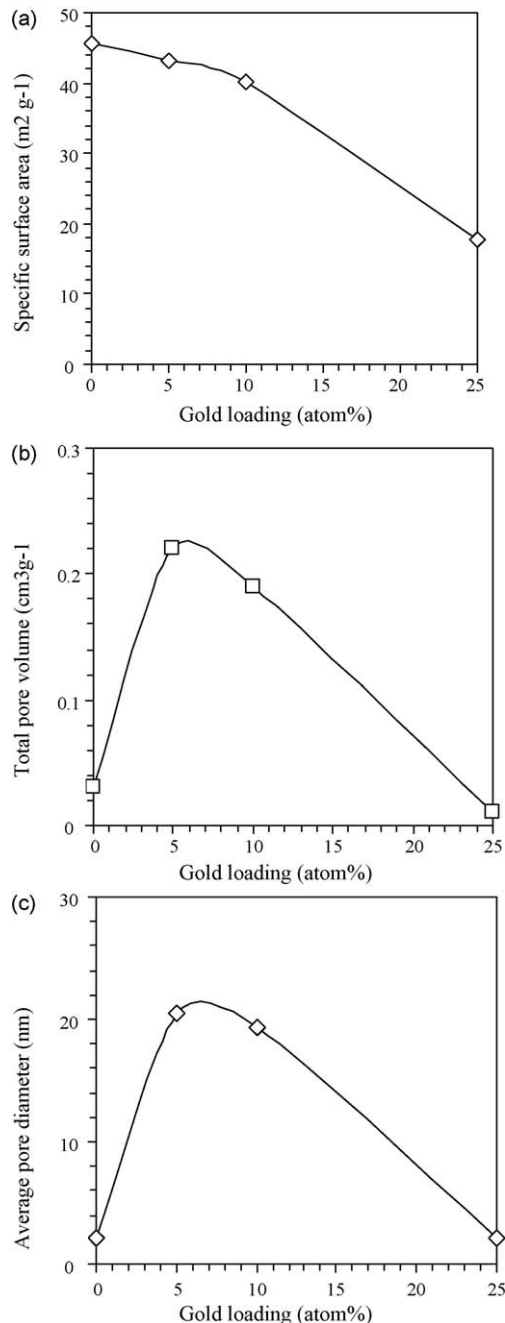


Fig. 2. Physicochemical properties of $\text{Au}/\text{Co}_3\text{O}_4$ catalysts with different Au loadings prepared by co-precipitation followed by calcination at 400 °C. (a) specific surface area, (b) total pore volume, (c) average pore diameter.

to air, they gradually disappeared with time on stream (TOS). For 10 at.% $\text{Au}/\text{Co}_3\text{O}_4$ catalyst, IR data shows no peaks assigned to $\text{HCo}(\text{CO})_4$ or $\text{Co}_2(\text{CO})_8$ species in the solution and no distinct change with TOS (Fig. 4c).

3.2. Catalytic results

3.2.1. Gold supported on different supports for the hydroformylation of 1-hexene

As shown in Table 1, Au/AC , $\text{Au}/\text{Al}_2\text{O}_3$, Au/TiO_2 , $\text{Au}/\text{Fe}_2\text{O}_3$, Au/ZnO , Au/CeO_2 and Au/PVP exhibits very low or no hydroformylation activities (Table 1, entries 1–7). The reactant 1-olefin introduced mainly remained unchanged and the major products were isomerized olefins or hydrogenated paraffin depending on

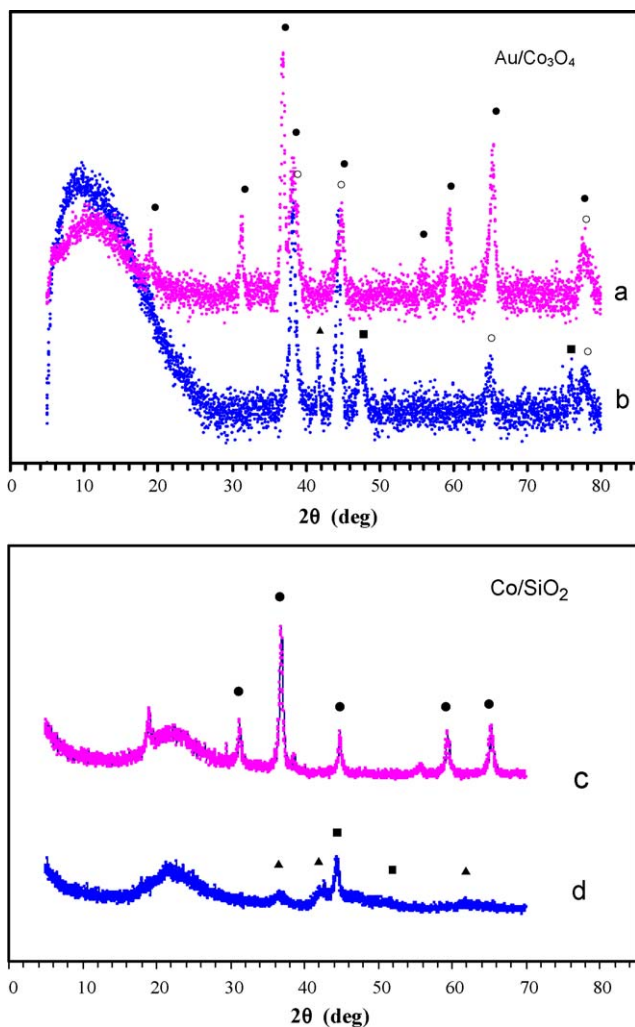


Fig. 3. X-ray diffraction patterns of 10 at.% Au/Co₃O₄ catalyst prepared by co-precipitation and 20 wt.% Co/SiO₂ catalyst prepared by impregnation. (a) before H₂ pretreatment; (b) after H₂ pretreatment (2.0 MPa, 100 °C, 3 h) in 2 ml *n*-heptane; (c) before H₂ reduction; (d) reduced in 80 ml/min H₂ flow at 400 °C for 3 h. (●) Co₃O₄; (▲) CoO; (■) Co; (○) Au.

the catalyst component and the reaction conditions. Tricobalt tetraoxide alone did not exhibit any activity for 1-hexene conversion (Table 1, entries 8 and 9). In contrast, very interestingly, supported nanoparticulate gold catalysts, 5 or 10 at.% Au/Co₃O₄, exhibit noticeably high hydroformylation activity (Table 1, entries 10–14, 16–18). Entries 10–12 show that the catalytic activity and selectivity to normal aldehyde increased with an increase in initial syngas pressure and the selectivity to aldehydes exceeded 80%. The effect of gold loadings was examined in entries 15–18 by using reduced amount of the catalyst (20 mg) with respect to entries 10–12 (50 mg), the catalytic activity is appreciably increased with increasing gold loading from 1 to 10 at.% and is notably decreased with a much higher gold loading of 25 at.%. Very low activity was observed for 1 at.% Au catalyst.

3.2.2. Effect of temperature on the hydroformylation of 1-hexene

Fig. 5 shows that, in the temperature range of 100–150 °C, the rate of hydroformylation is much faster than those of the hydrogenation of both 1-hexene and aldehydes formed and of the isomerization of 1-hexene, resulting in a high selectivity to aldehyde as described in Scheme 2. At temperatures above 150 °C, 1-hexene hydrogenation to *n*-hexane and especially isomerization to internal olefins are markedly promoted. At 170 °C, the Fischer-Tropsch (FT)

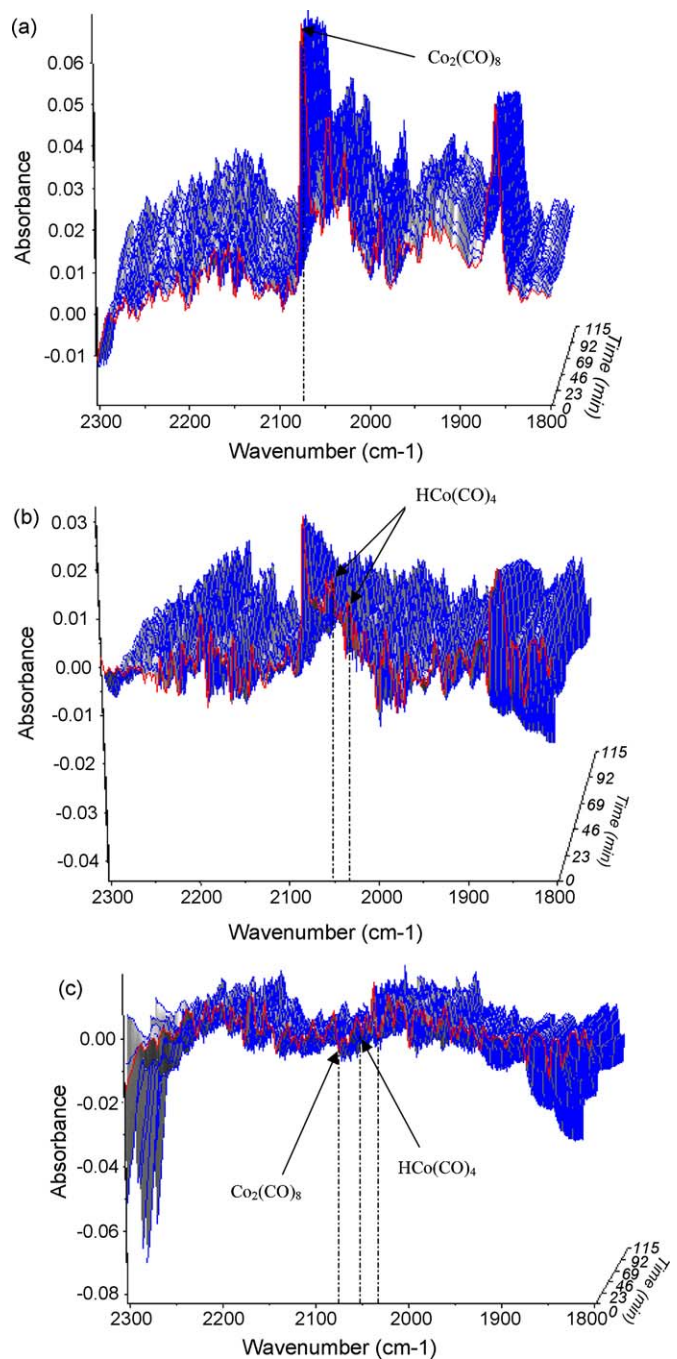


Fig. 4. IR spectroscopic data for (a) 40 mg $\text{Co}_2(\text{CO})_8$ in 2 ml *n*-heptane solution, (b) post-reaction mixture with 40 mg $\text{Co}_2(\text{CO})_8$, and (c) post-reaction mixture with 300 mg 10 at.% $\text{Au}/\text{Co}_3\text{O}_4$ catalyst. Reaction conditions: $P = 4 \text{ MPa}$; 1-hexene = 8 mmol; solvent *n*-heptane = 14 mmol; reaction time = 2 h; before reaction, the catalyst was pretreated with hydrogen (2.0 MPa, 100 °C, 3 h) in 2 ml *n*-heptane.

synthesis occurred to produce a series of compounds with higher molecular mass directly from syngas. If the temperature is further raised to 200 °C, the hydrogenation of olefin is enhanced while isomerization and hydroformylation are relatively depressed.

3.2.3. Hydroformylation of various olefins

Table 2 shows the performances of 5 at.% Au/Co₃O₄ for the hydroformylation of olefins with different molecular structures under the same reaction conditions. One can see that terminal olefins such as 1-hexene (**Table 2**, entry 1), methylenecyclohexane (**Table 2**, entry 5) and 3,3-dimethyl-1-butene (**Table 2**, entry 6) are

Table 1

Hydroformylation of 1-hexene over gold nanoparticles supported on activated carbon and on base metal oxides.

Entry	Catalyst (mg)	Au/(Au+M) (at.%)	Au or Co/1-hexene (molar ratio, 10^{-4})	Temperature/(H ₂ +CO pressure) (°C/MPa)	Conversion (%)	Reaction rate (h ⁻¹ mol hexene/mol Au)	Product selectivity (%)					<i>n/i</i> ^a
							<i>n</i> -Hexane	Internal olefins	Aldehydes	Alcohols	Heavy end	
1	Au/AC (35)	0.1	4.8 ^b	175/3.8	2.6	0.3	0.3	96.7	3.1	0	0	–
2	Au/Al ₂ O ₃ (200)	0.3	18.2 ^b	175/3.8	32.7	9.0	20.6	76.2	0.4	1.7	0.8	1.1
3	Au/TiO ₂ (40)	1.2	19.1 ^b	160/12.1	10.9	2.9	66.2	30.6	0	3.2	0	1.1
4	Au/Fe ₂ O ₃ (50)	5	52.4 ^b	195/3.8	22.2	4.9	8.3	82.8	0	8.8	0.1	3.1
5	Au/ZnO (50)	5	35.8 ^b	120/4	0.2	0.03	0	100	0	0	0	–
6	Au/CeO ₂ (50)	4.3	15.9 ^b	120/4	0.9	0.3	0	100	0	0	0	–
7	Au/PVP	–	47.6 ^b	120/4	0.1	0.01	0	0	0	0	0	–
8 ^c	Co ₃ O ₄ (50)	0	0.078	100/4	0	–	–	–	–	–	–	–
9	Co ₃ O ₄ (50)	0	0.078	140/4	0.5	–	–	–	–	–	–	–
10	Au/Co ₃ O ₄ (50)	5	0.069	100/3	46.7	6.4	0	5.7	88.6	2.1	3.6	1.6
11	Au/Co ₃ O ₄ (50)	5	0.069	100/4	81.8	11.3	0	5.8	87.5	3.1	3.6	2.1
12	Au/Co ₃ O ₄ (50)	5	0.069	100/5	90.1	12.4	0	4.9	87.8	3.7	3.6	2.6
13 ^d	Au/Co ₃ O ₄ (20)	10	0.023	130/4	99.5	52.4	0.3	5.4	83.9	4.4	5.9	1.2
14 ^c	Au/Co ₃ O ₄ (3)	10	0.003	130/4	88.2	56.7	0.2	11.9	81.5	2.4	3.9	1.2
15	Au/Co ₃ O ₄ (20)	1	0.030	100/4	0.4	0.7	0	13.9	81.2	2.0	2.9	1.1
16	Au/Co ₃ O ₄ (20)	5	0.028	100/4	19.6	6.8	0	6.5	88.3	1.7	3.6	2.2
17	Au/Co ₃ O ₄ (20)	10	0.023	100/4	60.3	8.7	0	3.3	91.2	2.6	3.0	2.3
18	Au/Co ₃ O ₄ (20)	25	0.017	100/4	33.6	2.9	0	4.7	91.6	1.5	2.2	2.3

Reaction conditions: reaction time = 20 h; 1-hexene 5.6 mmol, *n*-pentane 12.1 mmol (entries 1, 2, and 4); 1-hexene 3.2 mmol, *n*-pentane 6.9 mmol (entry 3); 1-hexene 8 mmol, *n*-heptane 14 mmol (entries 5–18).

^a *n/i*=linear-to-branched ratio of aldehydes **1**/(**2**+**3**) (entries 1, 10–18), linear-to-branched ratio of corresponding alcohols (entries 2, 3, and 4).

^b Molar ratio ($\times 10^{-4}$) of Au to substrate.

^c Reaction time = 30 h, hydrogen pretreatment (100 °C, 2.0 MPa, 3 h).

^d Reaction time = 5.5 h.

more reactive than internal olefins such as cyclohexene (Table 2, entry 4), which suggests the steric effects lead to preferential terminal insertion of CO over internal insertion. Compared with cyclohexene, *cis*-2-hexene and *cis*-3-hexene exhibited much higher reactivity (Table 2, entries 2 and 3) because of isomerization to 1-hexene, which resulted in the selectivity to aldehydes similar to that of 1-hexene (Scheme 2). The high selectivity to the formation of the terminal formyl group with methylenecyclohexane and 3,3-dimethyl-1-butene is attributable to the steric hindrance by substituent for their isomerization to internal olefins.

3.2.4. Effect of time on stream on reaction performances

As shown in Table 3 (entries 1 and 2, 3–6 and 7–8), the conversion of 1-hexene is gradually increased while aldehyde selectivity and normal-to-isomer ratio are maintained with time

Fig. 5. Effect of reaction temperature on the hydroformylation of 1-hexene over Au/Co₃O₄ catalyst prepared by co-precipitation followed by calcination at 400 °C. Reaction conditions: 10 at % Au/Co₃O₄ = 20 mg; *P* = 4 MPa; 1-hexene = 8 mmol; *n*-heptane = 14 mmol; reaction time = 5.5 h. Symbols for product selectivity: (○) *n*-Hexane; (□) Internal olefins; (●) Aldehydes; (◇) Alcohols; (△) Heavy end.

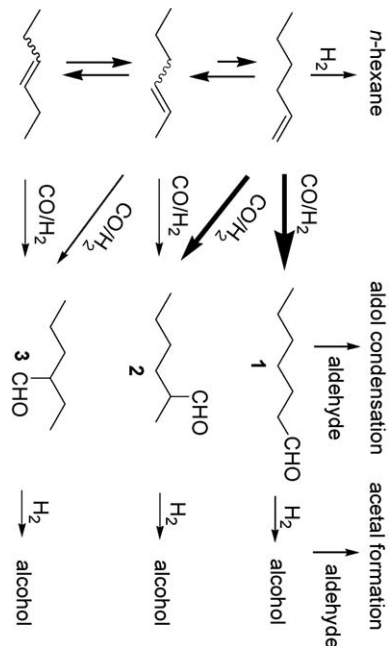
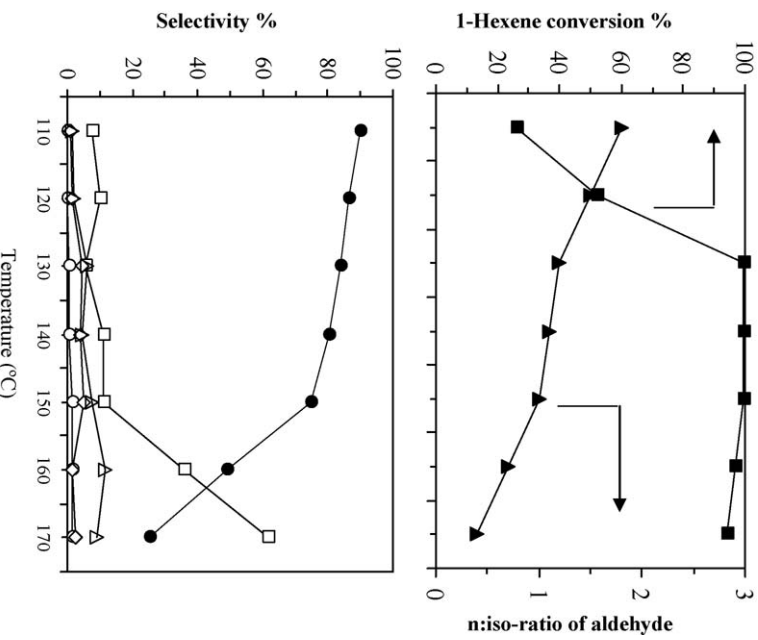
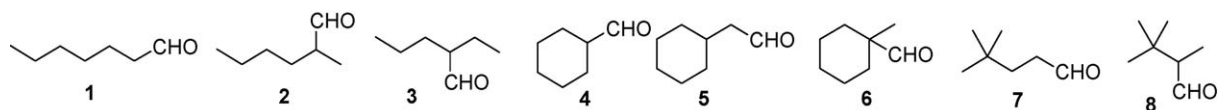


Table 2

Hydroformylation of olefins over Au/Co₃O₄ catalysts prepared by co-precipitation and by calcination at 400 °C.



Entry	Olefins	Conversion (%)	Selectivity (%)					n/i ^a
			Isomerized olefins	Aldehydes	Aldehyde isomer ratio	Alcohols	Heavy end	
1	1-Hexene	81.8	5.8	87.5	68.3:25.7:6.0 (1:2:3)	3.1	3.6	2.1
2	cis-2-Hexene	46.7 ^b	5.2	90.8	62.8:27.3:9.9 (1:2:3)	3.1	0.9	1.7
3	cis-3-Hexene	49.5 ^c	3.4	91.6	62.7:25.4:11.9 (1:2:3)	2.7	2.9	1.7
4	Cyclohexene	3.8	0	93.5	100 (4)	6.5	0	–
5	Methylenecyclohexane	35.7	15.7	84.3	80:0 (5:6) ^d	0	0	–
6	3,3-Dimethyl-1-butene	95.4	0	91.6	97:3 (7:8)	2.7	4.1	29 ^e

Reaction conditions: 5 at.% Au/Co₃O₄ = 50 mg; T = 100 °C; P = 4 MPa; olefin = 8 mmol (Co/olefin = 6.9 at.-%); solvent n-heptane = 14 mmol; reaction time = 20 h.

Bold values mean number of compound.

^a n/i = linear-to-branched ratio of aldehydes **1/(2+3)**.

^b Conversion to the products except for cis-2- and trans-2-hexene.

^c Conversion to the products except for cis-3- and trans-3-hexene.

^d Unidentified two aldehyde isomers except for **5** and **6** were formed in 13.9:6.1.

^e Ratio of **7/8**.

Table 3

Time-on-stream effect on hydroformylation of 1-hexene over Au/Co₃O₄ catalysts prepared by co-precipitation and by calcination at 400 °C.

Entry	Temperature (°C)	Time (h)	Catalyst weight (mg)	Hydrogen pretreatment	Conversion (%)	Selectivity (%)					n/i ^a
						Hexane	Internal olefins	Aldehydes	Alcohols	Heavy end	
1	100	20	20	No	60.3	0	3.3	91.2	2.6	3.0	2.3
2	100	55	20	No	92.6	0	3.3	86.3	4.2	6.2	2.2
3	130	5	3	Yes	10.3	0	17.4	80.9	0.3	1.4	1.2
4	130	10	3	Yes	40.2	0	15.7	81.9	0.9	1.6	1.2
5	130	20	3	Yes	72.9	0	16.1	79.5	1.6	2.7	1.2
6	130	30	3	Yes	88.2	0.2	11.9	81.5	2.4	3.9	1.2
7	130	5	20	Yes	95.2	0	12.3	81.9	2.4	3.4	1.3
8	130	5.5	20	Yes	99.5	0.3	5.4	83.9	4.4	5.9	1.2
9	130	20	20	Yes	100	0.1	0	14.5	27.8	57.6	0.5

Reaction conditions: 10 at.% Au/Co₃O₄; P_{initial synthesis gas} = 4 MPa; solvent n-heptane = 14 mmol; 1-hexene = 8 mmol; for entries 3–9, catalyst was pretreated under the conditions of 100 °C, 2 MPa and 3 h.

^a n/i = linear-to-branched ratio of aldehydes.

on stream (TOS). As shown by entries 8 and 9, further extension of reaction time resulted in the complete conversion of olefin but caused acetal formation. As described in Scheme 2, the heavy by-product acetals and derivatives are produced from the reaction of aldehyde with alcohol. Before complete conversion of the olefin, the catalytic sites (Au or Co) might be occupied with olefins to catalyze its hydroformylation. After the consumption of olefin, the free catalytic sites may adsorb aldehydes to form alcohols, which reacts with aldehydes to give acetals. For both aldehyde hydrogenation and subsequent acetal formation, the normal aldehydes are always more reactive than the branched aldehydes owing to smaller steric hindrance, which results in a decrease in normal-to-isomer ratio with TOS. Accordingly, it is important to control olefin conversion for higher selectivity to desired aldehydes.

Fig. 6 shows the reaction rates at 100 °C of 1-hexene hydroformylation over 10 at.% Au/Co₃O₄ catalyst pretreated in hydrogen (2.0 MPa, 100 °C, 3 h) after calcination at 400 °C. A plot of $\ln[1-x]$ vs. time *t* gives a straight line with a slope of *k* (rate equation obtained was $\ln[1-x] = -0.08t + 0.286$), which suggests that the hydroformylation of 1-hexene is a first order reaction with respect to the concentration of 1-hexene. Here: [x] is the conversion of 1-hexene; *k* is the first order rate constant. It should be noted that even if the catalyst was reduced with H₂ before run, relatively long induction period of around 4 h was observed to start the hydroformylation reaction.

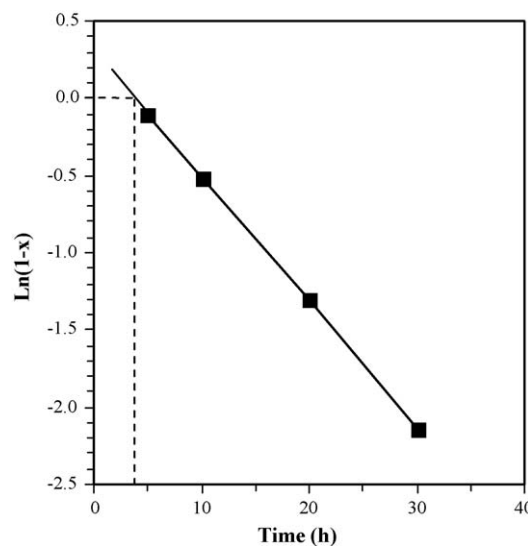


Fig. 6. Reaction rates for hydroformylation of 1-hexene (x: conversion% of 1-hexene). Reaction conditions: 10 at.% Au/Co₃O₄; P_{initial synthesis gas} = 4.0 MPa; solvent n-heptane = 14.0 mmol; 1-hexene = 8.0 mmol; catalyst was pretreated with hydrogen (100 °C, 2 MPa, 3 h) before run.

Table 4

Effect of catalyst pretreatment on hydroformylation of 1-hexene over Au/Co₃O₄ catalysts prepared by co-precipitation and by calcination at 400 °C.

Entry	Catalyst	Pretreatment			Conversion (%)	Selectivity (%)				η/i^a
		Temperature (°C)	Hydrogen pressure (atm)	Time (h)		Hexane	Internal olefins	Aldehydes	Alcohols	
1	Co ₃ O ₄	No treatment	0	—	—	—	—	—	—	—
2	Co ₃ O ₄ ^b	400	1	3	0	—	—	—	—	—
3	5 at.% Au/Co ₃ O ₄	No treatment	19.6	0	6.5	88.3	1.7	3.6	2.2	—
4	5 at.% Au/Co ₃ O ₄ ^c	100	20	3	81.8	0	5.8	87.5	3.1	3.6
5	5 at.% Au/Co ₃ O ₄ ^c	125	20	3	76.5	0	3.4	88.1	3.3	6.2
6	5 at.% Au/Co ₃ O ₄ ^c	150	20	6	75.1	0	2.8	87.8	2.6	6.8
7	10 at.% Au/Co ₃ O ₄	No treatment	60.3	0	3.3	91.2	2.6	3.0	2.3	2.1
8	10 at.% Au/Co ₃ O ₄ ^d	100	20	3	93.3	0	5.2	85.5	3.6	5.6
										2.2

Reaction conditions: catalyst = 20 mg; T = 100 °C; P_{initial synthesis gas} = 4 MPa; solvent n-heptane = 14 mmol; olefin = 8 mmol; reaction time = 20 h;

^a η/i = linear-to-branched ratio of aldehydes;

^bCatalysts were reduced in a glass tube in a pure hydrogen flow of 40 ml/min under atmospheric pressure;

^{c,d}Catalysts were pretreated in 2 ml n-heptane.

Table 5

Hydroformylation of 1-hexene over silica-supported cobalt or cobalt-gold catalysts prepared by impregnation and by calcination and reduction at 400 °C.

Entry	Catalyst	Catalyst preparation			Conversion (%)	Selectivity (%)				η/i^a
		Gold precursor	Solution	Impregnation method		Hexane	Internal olefins	Aldehydes	Alcohols	
1	Co/SiO ₂	—	H ₂ O	—	54.6	0	4.3	91.4	2.3	2.0
2 ^b	Co/Au/SiO ₂	Au(CH ₃) ₂ (acac)	Ethanol	Sequential impregnation	53.7	0	3.9	91.5	2.2	2.4
3	Co/SiO ₂	—	Ethanol	—	66.0	0	3.8	84.0	3.2	8.9
4	Co-Au/SiO ₂	Au(CH ₃) ₂ (acac)	Ethanol	Co-impregnation	70.6	0	3.9	85.4	3.1	7.7
5	Co-Au/SiO ₂	AuCl ₃	H ₂ O	Co-impregnation	43.5	0	4.0	88.8	3.5	3.7
6	Co-Au/SiO ₂	HAuCl ₄ ·4H ₂ O	H ₂ O	Co-impregnation	43.4	0	5.1	89.3	2.3	3.4

Reaction conditions: catalyst 50 mg; (20 wt.-% Co loading, atom ratio of Co:Au = 19:1); T = 100 °C; P_{initial synthesis gas} = 4 MPa; solvent n-heptane = 14 mmol; 1-hexene = 8 mmol; catalyst was reduced in a glass tube in a hydrogen flow of 40 ml/min under atmospheric pressure at 400 °C for 3 h.

^a η/i = linear-to-branched ratio of aldehydes;

^bThe Co/Au/SiO₂ was prepared by impregnating Au(CH₃)₂(acac) in ethanol with Co/SiO₂ used in entry 1 and then calcined at 400 °C for 4 h. Gold loading was 5 at.-% of Au to (Au + Co).

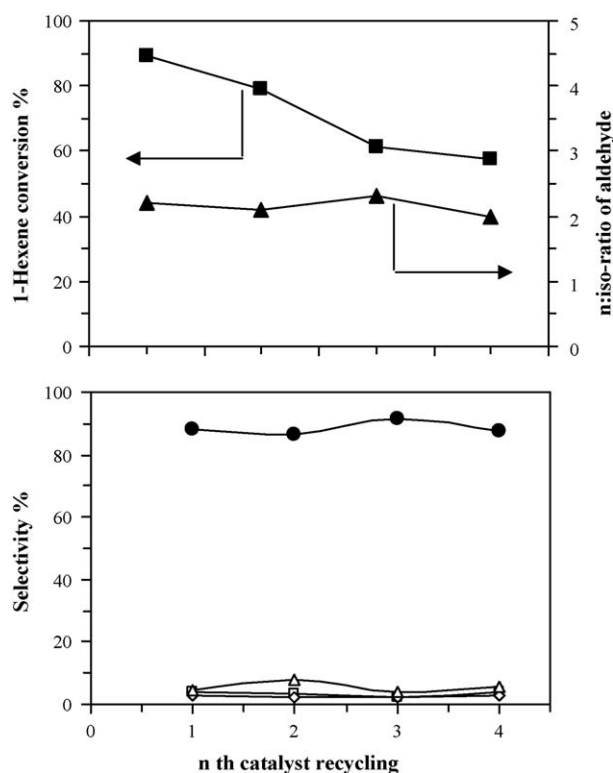


Fig. 7. Recycle use of Au/Co₃O₄ catalyst for the hydroformylation of 1-hexene. Reaction conditions: 5 at.% Au/Co₃O₄ prepared by co-precipitation followed by calcination at 400 °C = 20 mg; T = 100 °C; P = 4 MPa; 1-hexene = 8 mmol; solvent n-heptane = 14 mmol; reaction time = 20 h; the catalyst was pretreated with hydrogen (2 MPa, 100 °C, 3 h) before the first run; H₂ treatment was not repeated in 2–4 runs. Symbols for product selectivity: (□) internal olefins; (●) aldehydes; (△) alcohols; (◇) heavy end.

3.2.5. Effect of pretreatment of catalyst by hydrogen

Table 4 shows the effect of pretreatment of Co₃O₄ and Au/Co₃O₄ catalysts on hydroformylation of 1-hexene. Tricobalt tetraoxide without Au exhibited no catalytic activity irrespective of pre-reduction in a stream of hydrogen of 40 ml/min at atmospheric pressure or under 2.0 MPa hydrogen at 100 °C for 3 h in n-heptane solvent. In contrast, the activity of Au/Co₃O₄ for olefin hydroformylation was remarkably improved from 19.6% to 70–80% (entries 3–6) or from 60.3% to 93.3% (entries 7 and 8) with hydrogen pretreatment before reaction.

3.2.6. Recycle use of Au/Co₃O₄ catalyst

A major advantage of heterogeneous catalysts over homogeneous catalysts is facile catalyst separation and recycle use. Industrial cobalt-catalyzed hydroformylation transforms cobalt carbonyl catalysts into insoluble or water-soluble cobalt complexes or cobalt precipitates due to the instability of cobalt carbonyl under reduced syngas pressure and at elevated temperature. The materials recovered require complicated catalyst regeneration processes. In contrast, catalyst separation and recycle use (four times) of the Au/Co₃O₄ catalyst by simple decantation were successfully carried out (**Fig. 7**), even though liquid phase was vigorously stirred during the reaction. Only a slight decrease in catalytic activity was observed along with an increase in the recycle run from the third run.

3.2.7. Hydroformylation reaction by Co/SiO₂ and Au-Co/SiO₂ catalyst

The catalytic performances of Co/SiO₂ and Au-Co/SiO₂ catalyst are shown in **Table 5**. One can see that Au nanoparticles dispersed on Co/SiO₂ by impregnating Au(CH₃)₂(acac) in ethanol did not improve the catalytic activity (**Table 5**, entries 1 and 2). Supported Co₃O₄ was fully reduced to Co metal at 400 °C as shown in **Fig. 3(c and d)**. Co-impregnated Au-Co₃O₄/SiO₂ catalyst using dimethyl Au(III) acetylacetone as a gold precursor could exhibit better catalytic performances for hydroformylation reaction (**Table 5**,

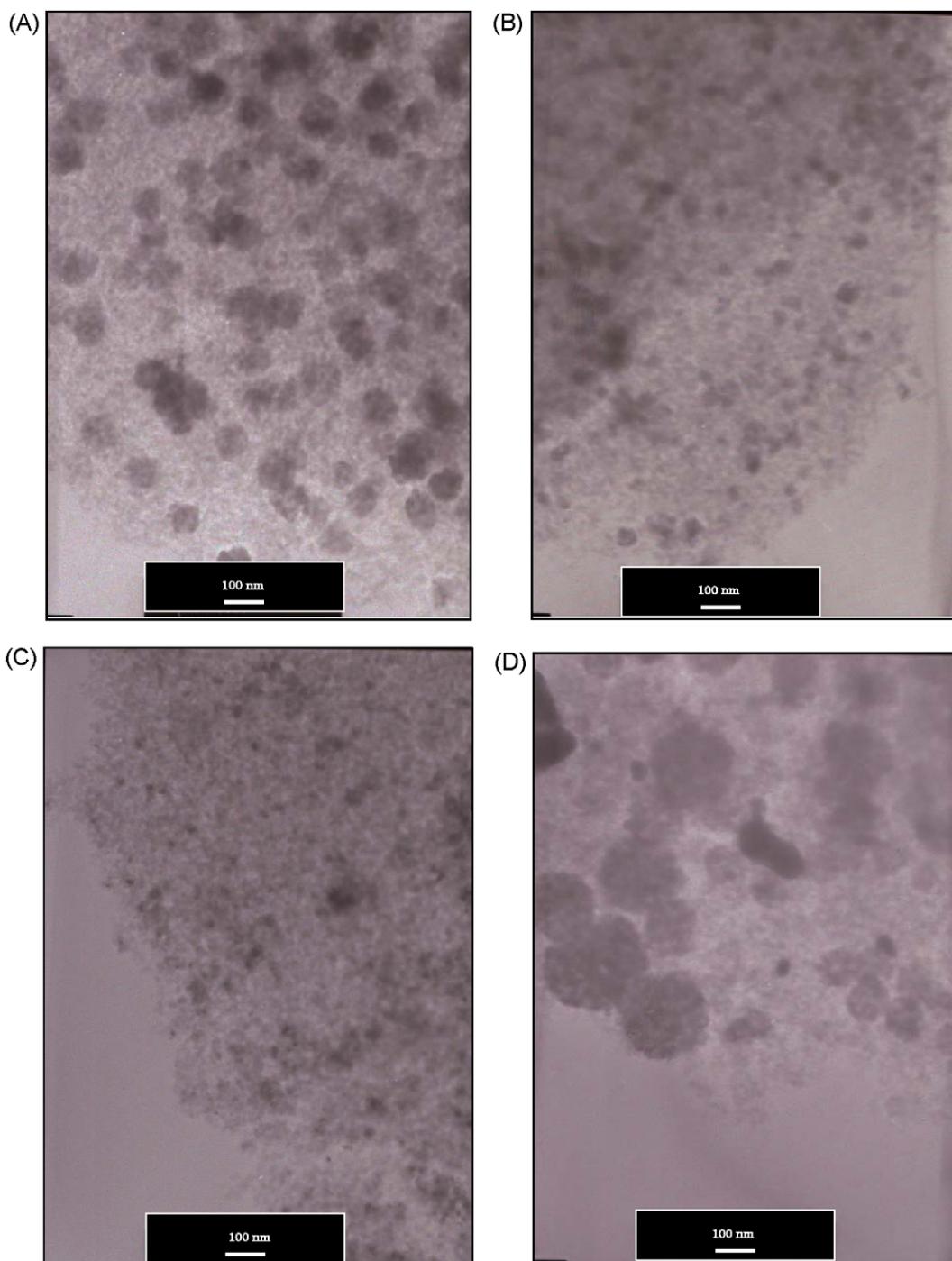


Fig. 8. TEM images of the Co/SiO₂ or Au-Co/SiO₂ catalysts (20 wt.% Co loading, atom ratio of Co:Au = 19:1) prepared by different gold precursors and impregnating solutions followed by calcinations at 400 °C. (A) Co/SiO₂ (H₂O); (B) Co/SiO₂ (ethanol); (C) Au-Co/SiO₂ (Au(CH₃)₂(acac); ethanol); (D) Au-Co/SiO₂ (HAuCl₄·4H₂O; H₂O).

entries 1 and 4) owing to smaller cobalt crystal sizes (Fig. 8A and C). The Au-Co₃O₄/SiO₂ catalyst prepared by co-impregnation with cobalt nitrate and HAuCl₄ aqueous solution was composed of much larger Co₃O₄ crystal size (Fig. 8D). The above results showed that after reduction at 400 °C the crystal size of metallic Co determined the catalytic activity for hydroformylation while the coexisting Au nanoparticles did not interfere the reaction over Co particles.

4. Discussion

Taking into account the catalytic activity order in hydroformylation widely accepted (Rh > Co > Ir > Ru > Os > Pt > Pd >

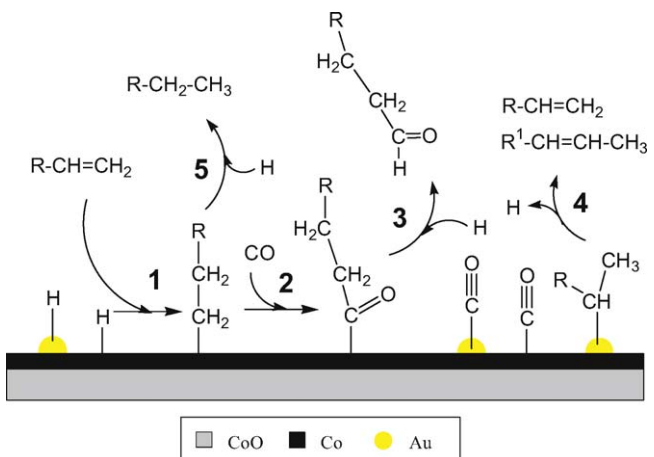
Fe > Ni, ...) [1c], we can assume that the markedly enhanced catalytic activity of Au/Co₃O₄ compared to Co₃O₄ or other supported Au nanoparticles (Au on AC, PVP, Al₂O₃, TiO₂, Fe₂O₃, ZnO and CeO₂) is ascribed to Co⁰ metal particles, which are formed on the surface of cobalt oxides by spillover hydrogen from gold nanoparticles.

To elucidate the active sites in this catalytic system, the performance of 5 at.% Au/Co₃O₄ catalyst was investigated after the pretreatment with hydrogen (H₂ pressure 2.0 MPa, 100 °C and 3 h). Appreciable improvement was observed from 19.6% (Table 1, entry 16) to 89.1% (first run in Fig. 7) under the same reaction conditions in 1-hexene conversion by H₂ pretreatment. A similar,

but a smaller effect of hydrogen pretreatment was observed with 10 at.% Au/Co₃O₄ catalyst (Table 4, entries 7 and 8). As shown in Fig. 3, the XRD patterns of 10 at.% Au/Co₃O₄ pretreated under H₂ pressure 2.0 MPa at 100 °C for 3 h show the formation of Co and CoO and the absence of Co₃O₄. Accordingly, the active sites may be Co metal or leached Co forming cobalt carbonyls that catalyze the homogeneous hydroformylation of 1-hexene. The recycle experiments confirmed that the active species was not HCo(CO)₄ formed by leaching but Co fixed metal on the surfaces of Au/Co₃O₄ catalysts. As shown in Fig. 7, the 1-hexene conversion in the forth cycle, 59%, is still much higher than that for a fresh catalyst without hydrogen pretreatment even though recycle experiments were carried out by simple decantation without subsequent hydrogen reduction. A hypothesis is that active sites are provided by metallic Co by immediate IR analysis of the reaction mixtures by comparison between the Co₂(CO)₈ and Au/Co₃O₄ catalytic system at similar 1-hexene conversions and at the same temperature and reaction time. As shown in Fig. 4, in the case of homogeneous Co₂(CO)₈ catalytic system, the peak at 2070 cm⁻¹ and the peaks at 2050 and 2030 cm⁻¹ can be assigned to Co₂(CO)₈ and HCo(CO)₄ species [33], respectively, which are obviously observable and gradually disappeared with time on stream (TOS) of 2 h. In contrast, with Au/Co₃O₄ catalyst, the IR data shows no peaks assigned to HCo(CO)₄ or Co₂(CO)₈ species in the solution and no distinct change with TOS. These results further support a possibility that the active species is solid Co⁰ metal crystal. The catalytic behaviour of co-precipitated Au/Co₃O₄ and Co supported on SiO₂ is similar to that of Co metal. The reaction of olefin with syngas shifts from hydroformylation to isomerization, and then to hydrogenation with elevated reaction temperature from 100 to 200 °C. This type of “reaction transition” with temperature suggests that the strength and structure of chemical adsorption of reactant molecules determines reaction pathways. Carbon monoxide can chemisorb on Co metal to form carbonyl complexes in two common forms: (1) the linear single M–CO bond, and (2) the bridged, in which the carbon atom, rehybridised to sp², makes σ bonds to two metal atoms. In addition, the molecule can also be dissociated to form cobalt carbide and oxygen species [34]. For the hydroformylation of olefins, the threshold temperature for carbonyl formation must lie below that for the formation of cobalt carbide, which requires the cleavage of carbon–oxygen bond. Furthermore, the linear CO adsorption is favourable for carbonyl formation. It is well established that hydroformylation mechanism involves olefin–metal complexation, formation of alkyl group (Scheme 3, pathway 1), transformation of the alkyl group to an acyl group (Scheme 3, pathway 2), and subsequent hydride transfer to aldehyde products (Scheme 3, pathway 3) [35]. If CO adsorbed does not favour going into alkyl group to give an acyl group, the hydroformylation may not proceed smoothly. The reaction will terminate at the second step followed by dehydrogenation to isomerized olefins or original olefin (Scheme 3, pathway 4) or by hydrogenation to paraffin (Scheme 3, pathway 5). Once the cobalt carbide is formed, the hydrogenation of cobalt carbide to methylene species (monomer unit) and subsequent methylene polymerization will occur to produce a wide FT products mainly consisting of linear hydrocarbons.

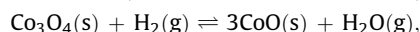
In Au/Co₃O₄-catalyzed hydroformylation reaction, the major role of Au nanoparticles might be *in-situ* reducing Co₃O₄ to Co metal under mild reaction conditions (3–5 MPa, 100–130 °C) [34,36]. Gold nanoparticles neither promote the catalytic activity by synergistic effects with Co metal nor interfere the hydroformylation reaction over Co metal.

The temperature programmed reduction (TPR) experiment, carried out by Andreeva et al., indicated the reduction of Co₃O₄ in Au/Co₃O₄ to elemental cobalt by aid of Au nanoparticles took place at a temperature about 200 °C lower than the reduction

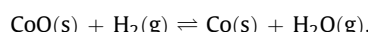


Scheme 3. Probable reaction pathways for the hydroformylation of olefins over Au/Co₃O₄ catalyst.

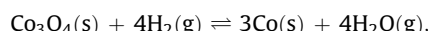
temperature for pure Co₃O₄ (350–370 °C) [36]. In general, two steps were involved in reducing Co₃O₄ to Co metal. The first step (1) represents the Co₃O₄ reduction to CoO. The second step (2) represents the CoO reduction to Co metal. Thermodynamic calculation (thermodynamic properties of Co₃O₄ and CoO obtained from [37]) showed that the reduction of Co₃O₄ to CoO or Co metal is exothermic reaction and the entropy of formation of CoO or Co metal is $\Delta_f H = -41.3$ or -3.5 kJ mol^{-1} at 25 °C and 1 atm. The corresponding values of $\Delta_f G$ in units kJ mol^{-1} for the step (1) and (2) are negative (-63.9 and -14.1 , respectively) at 25 °C and 1 atm, which suggests that the reduction of Co₃O₄ is thermodynamically favourable at room temperature and the formation of CoO is easier compared to its further reduction to Co metal. This is also consistent with our experimental data that only CoO and Co peaks but not Co₃O₄ to XRD diffraction in Fig. 3(a and b) were observed while the Au/Co₃O₄ was pretreated in *n*-heptane under mild conditions (2.0 MPa H₂, 120 °C, and 3 h).



$$\Delta G(\text{kJ mol}^{-1}, 25^\circ\text{C}) - 63.9, -41.3 \quad (1)$$



$$\Delta G(\text{kJ mol}^{-1}, 25^\circ\text{C}) - 14.1, -3.5 \quad (2)$$



$$\Delta G(\text{kJ mol}^{-1}, 25^\circ\text{C}) - 106.1, -51.8 \quad (3)$$

In the case of Au-Co/SiO₂ catalyst prepared by co-impregnation method, higher catalytic activity was obtained than Co/SiO₂ catalyst (Table 5, entries 3 and 4). This enhancement could be ascribed to higher dispersion of cobalt in the presence of gold (Fig. 8B and C).

5. Conclusions

Heterogeneous Co-based catalysts were prepared for the liquid phase hydroformylation of olefins and the following conclusions were obtained.

1. Gold nanoparticles deposited on Co₃O₄ catalyst are applicable to the heterogeneous hydroformylation of olefins under mild conditions (100–140 °C, 3–5 MPa). The selectivity was above 85% to desired aldehydes. The major role of gold nanoparticles is assumed to provide spillover H to reduce *in-situ* Co₃O₄ to Co metal at moderate reaction rates, so that Co crystals can remain as small nanoparticles

2. With increasing temperature, the reaction of olefins gradually shifts from hydroformylation to isomerization, and then to hydrogenation.
3. Cobalt nanoparticles are mainly responsible for hydroformylation and therefore highly dispersed metallic Co over SiO_2 surfaces can also exhibit good catalytic performances. The alloy formation of Au and Co, their interface effect, or spillover H from gold to cobalt or vice versa has only marginal effect on hydroformylation reaction.
4. The activity and selectivity of hydroformylation reaction are remarkably dependent on the molecular structure of olefin. In general, internal insertion takes place much slower than terminal insertion.
5. The Au/ Co_3O_4 catalysts can be recycled at least four times by simple decantation and are advantageous over homogeneous catalysts in process handling.

Acknowledgements

The authors are grateful to Prof. T. Ishida and Dr. Y. B. Yu of Tokyo Metropolitan University and Prof. T. Tsukuda of Hokkaido University for their help in catalyst preparation and useful discussions. They are also indebted to Prof. J. Inanaga and Prof. H. Furuno, Prof. T. Katsuki, Prof. H. Kitagawa and Dr. M. Yamauchi of Kyushu University for the measurements by IR, NMR, and XRD, respectively. Their acknowledgements are also extended to Mitsubishi Chemical Co. Ltd. for financial support.

References

- [1] (a) B. Cornils, in: J. Falbe (Ed.), *New Syntheses with Carbon Monoxide*, Springer-Verlag, Berlin, 1980;
- (b) C.A. Tolman, J.W. Faller, in: L. Pignolet (Ed.), *Homogeneous Catalysis with Metal Phosphine Complexes*, Plenum, London, 1983;
- (c) C.D. Frohning, C.W. Kohlpaintner, H.-W. Bohnen, in: B. Cornils, W.A. Herrmann (Eds.), *Applied Homogeneous Catalysis with Organometallic Compounds*, Wiley-VCH, Weinheim, 2002, pp. 31–85.
- [2] W.A. Herrmann, B. Cornils, *Angew. Chem. Int. Ed.* 36 (1997) 1049–1067.
- [3] M.E. Broussard, B. Juma, S.G. Train, W.-J. Peng, S.A. Laneman, G.G. Stanley, *Science* 260 (1993) 1784–1788.
- [4] F.R. Hartley, D.J.A. McCaffrey, S.G. Murray, P.N. Nicholson, *J. Org. Chem.* 206 (1981) 347–359.
- [5] C.-G. Jia, Y.-P. Wang, H.-Y. Feng, *React. Polym.* 18 (1992) 203–211.
- [6] F. Shibahara, K. Nozaki, T. Hiyama, *J. Am. Chem. Soc.* 125 (2003) 8555–8560.
- [7] Y. Zhang, K. Nagasaka, X.Q. Qiu, N. Tsubaki, *Appl. Catal.* 276 (2004) 103–111.
- [8] B.T. Li, X.H. Li, K. Asami, K. Fujimoto, *Energy Fuels* 17 (2003) 810–816.
- [9] Y. Zhang, K. Nagasaka, X.Q. Qiu, N. Tsubaki, *Catal. Today* 104 (2005) 48–54.
- [10] T.A. Kainulainen, M.K. Niemelä, A.O.I. Krause, *J. Mol. Catal.* 122 (1997) 39–49.
- [11] X.Q. Qiu, N. Tsubaki, Sh.L. Sun, K. Fujimoto, *Catal. Commun.* 2 (2001) 75–80.
- [12] A.S.K. Hashmi, G.J. Hutchings, *Angew. Chem. Int. Ed.* 45 (2006) 7896–7936.
- [13] A. Stephen, K. Hashmi, *Chem. Rev.* 107 (2007) 3180–3211.
- [14] M. Haruta, T. Kobayashi, H. Sano, N. Yamada, *Chem. Lett.* (1987) 405–408.
- [15] M. Haruta, K. Saika, T. Kobayashi, S. Tsubota, Y. Nakahara, *Chem. Express* 3 (1988) 159–162.
- [16] T. Hayashi, K. Tanaka, M. Haruta, *J. Catal.* 178 (1998) 566–575.
- [17] M. Haruta, *Chem. Rec.* 3 (2003) 75–87.
- [18] D. Andreeva, V. Idakiev, T. Tabakova, A. Andreev, *J. Catal.* 158 (1996) 354–355.
- [19] J.K. Edwards, B.E. Solsona, P. Landon, A.F. Carley, A. Herzing, C.J. Kiely, G.J. Hutchings, *J. Catal.* 236 (2005) 69–79.
- [20] F. Besenbacher, I. Chorkendorff, B.S. Clausen, B. Hammer, A.M. Molenbroek, J.K. Nørskov, I. Stensgaard, *Science* 279 (1998) 1913–1915.
- [21] M.Sh. Chen, D. Kumar, Ch.-W. Yi, D.W. Goodman, *Science* 310 (2005) 291–293.
- [22] J. Guzman, S. Garrettin, J.C. Fierro-Gonzalez, Y.L. Hao, B.C. Gates, A. Corma, *Angew. Chem. Int. Ed.* 44 (2005) 4778–4781.
- [23] A. Abad, P. Concepción, A. Corma, H. García, *Angew. Chem. Int. Ed.* 44 (2005) 4066–4069.
- [24] F. Bocuzzi, A. Chiorino, M. Manzoli, P. Lu, T. Akita, S. Ichikawa, M. Haruta, *J. Catal.* 202 (2001) 256–267.
- [25] H. Sakurai, A. Ueda, T. Kobayashi, M. Haruta, *Chem. Commun.* (1997) 271–272.
- [26] R.S. Yolles, B.J. Wood, H. Wise, *J. Catal.* 21 (1971) 66.
- [27] H. Sakurai, M. Haruta, *Appl. Catal. A* 127 (1995) 93–105.
- [28] X.H. Liu, M. Haruta, M. Tokunaga, *Chem. Lett.* 37 (2008) 1290–1291.
- [29] H. Tsunoyama, H. Sakurai, N. Ichikuni, Y. Negishi, T. Tsukuda, *Langmuir* 20 (2004) 11293–11296.
- [30] M.S. Niasari, F. Davar, M. Mazaheri, M. Shaterian, *J. Magn. Magn. Mater.* 320 (2008) 575–578.
- [31] X.H. Liu, W.S. Linghu, X.H. Li, K. Asami, K. Fujimoto, *Appl. Catal. A: Gen.* 303 (2006) 251–257.
- [32] J.L. Gu, W. Fan, A. Shimojima, T. Okubo, *J. Solid State Chem.* 181 (2008) 957–963.
- [33] Yu T. Vigranenko, V.A. Rybakov, V.V. Kashina, B.P. Tarasov, *Kinet. Catal.* 37 (1996) 524–527 (Translated from *Kinetika i Kataliz*, 37 (1996) 558).
- [34] G.C. Bond, C. Louis, D.T. Thompson, *Catalysis by Gold*, Imperial College Press, 2006 (Chapter 5, pp. 137, 151).
- [35] M. Beller, in: K.-D. Wiese, D. Obst (Eds.), *Catalytic Carbonylation Reactions*, Springer-Verlag Berlin Heidelberg, 2006, pp. 5–6.
- [36] L.I. Ilieva, G. Munteanu, D.Ch. Andreeva, *Bulg. Chem. Commun.* 30 (1998) 378–382.
- [37] K.H. Lemke, R.J. Rosenbauer, J.L. Bischoff, D.K. Bird, *Chem. Geol.* 254 (2008) 136–144.